# The Influence of a Top Cover on the Leakage from Microstrip Line

F. Mesa, A. A. Oliner, *Life Fellow, IEEE*, D. R. Jackson, *Fellow, IEEE*, and Manuel J. Freire

***Abstract*—When a microwave integrated circuit is enclosed in a package, the top cover causes the transmission lines used in the circuit to become leaky at a *lower* frequency than otherwise. This effect is investigated in detail for microstrip line, and is found to be particularly dramatic. The leakage is strong enough to produce spurious effects that can ruin the performance of the circuit. The amplitude behavior is obtained by numerically solving for the current on a covered microstrip line due to a delta-gap source excitation. The results clearly show that a strong leaky mode (LM) is excited and that spurious effects due to the LM and from direct radiation from the source generally become more severe at higher frequencies and when the top cover is brought nearer to the strip.**

***Index Terms*—Leaky waves, microstrip, packaging effects, printed circuits, stripline, transmission lines.**

## I. Introduction

MUCH IS already known about leaky dominant modes on various printed-circuit transmission lines, where the leakage occurs in the form of a surface wave on the surrounding substrate [1]–[21]. The presence of the leakage can cause power loss, crosstalk, and spurious interference effects when the line is used in a microwave integrated circuit [13], [16], [21]. Almost all of these studies have assumed that the lines are isolated, and that any sidewall or top cover is located far away. In practice, however, these lines are used in microwave circuits, which, in turn, are placed into packages of some type. It is, therefore, important to determine the influence of the top covers and sidewalls of a package on the possible leakage behavior of various transmission lines. Previous papers [11], [15], [18] have considered structures similar to covered microstrip, but did not explicitly examine the influence of the top cover on the leakage. However, an important first step in this direction has appeared recently in [22].

With respect to the influence of a top cover, which is the subject of this paper, [22] showed that the principal effect is to ***lower*** the frequency at which leakage begins. When the top cover is brought near to the line, the reduction in frequency at which the leaky mode (LM) appears can be large enough to be of serious concern. The example treated in [22] was that of coplanar waveguide (CPW). We have found in this study that, when the line is a ***microstrip line***, the effect of a top cover on leakage is even more dramatic. For a microstrip line without a top cover, a bound (conventional) dominant mode is present at all frequencies, but ***in addition***, a dominant (quasi-TEM) LM exists at higher frequencies, when the substrate thickness is typically one-tenth of a wavelength or more [16]. As shown here, however, the presence of a top cover (Fig. 1) can lower very significantly the frequency at which leakage begins. For a sufficiently small cover height, in fact, it is found that leakage occurs at ***all frequencies***.

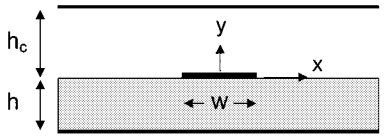


Fig. 1. Geometry of an infinite microstrip transmission line with a top cover (perfectly conducting plane).

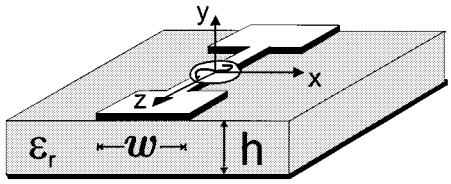


Fig. 2. Geometry of an infinite microstrip line excited by a delta-gap voltage source at $z = 0$.

In Section II, we first review the properties of the leaky dominant mode on microstrip line, and then point out what happens to the dispersion curve for the surface wave (which becomes a parallel-plate mode due to the presence of the top cover) when the top cover is brought near to the line. This behavior explains why the leakage frequency is lowered as the top cover is brought close to the substrate.

In Section III, the methods of analysis that are used to explore the properties of the LM and its excitation are discussed. The analysis assumes a unit-amplitude delta-gap voltage source on a microstrip line of infinite length (Fig. 2). A semianalytical spectral-domain technique is used to solve for the current on the conducting strip due to the source excitation, and then to resolve this into its two basic components, the current of the bound mode (BM) and the current of the continuous spectrum (CS). The CS current is, in turn, resolved into the physical LM current and a remainder part called the residual-wave (RW) current. The RW current corresponds primarily to the direct radiation from the source.

In Section IV, we present the results from our calculations, starting with dispersion plots that demonstrate very clearly that the onset of leakage is dramatically lowered in frequency when a top cover is brought near to the microstrip line. Plots of the

Manuscript received March 5, 2000; revised August 21, 2000.

F. Mesa and M. J. Freire are with the Microwave Group, Department of Electronics and Electromagnetism, University of Seville, 41012 Seville, Spain.

A. A. Oliner is with the Department of Electrical Engineering, Polytechnic University, Brooklyn, NY11201 USA.

D. R. Jackson is with the Department of Electrical and Computer Engineering, University of Houston, Houston, TX 77204-4793 USA.

Publisher Item Identifier S 0018-9480(00)10711-2.

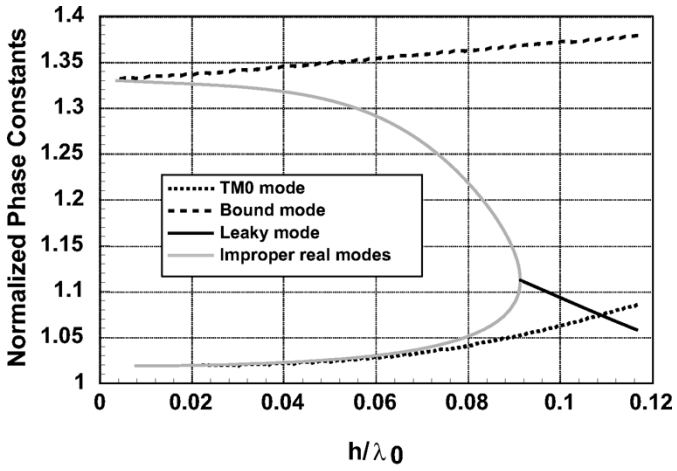


Fig. 3. Dispersion plot showing the normalized phase constant $\beta/k_0$ versus normalized frequency $h/\lambda_0$ for an open microstrip line (top cover in Fig. 1 is at infinity). The strip-width-to-substrate ratio $w/h$ is unity, and the substrate relative permittivity is $\varepsilon_r = 2.2$. The LM is shown as a solid black line, with the real improper solutions shown as gray lines. The BM is represented by a dashed line, and the dispersion curve for the $\mathrm{TM}_0$ parallel-plate mode of the background structure is shown by a dotted line. It is seen that, at higher frequencies, an LM is present in addition to the conventional BM. The real improper solutions in gray are nonphysical.

current on the microstrip line versus distance from the source are then presented, in order to clearly establish how spurious transmission effects may be caused by the LM, or by the CS, in general, and how these effects become more severe as the cover height is lowered or the frequency is increased. We show that the amplitude of the LM may be quite large, and that its presence may produce significant spurious transmission effects. The generalized pencil of functions (GPOF) method is used as a tool to help in the further quantification of the LM excitation, by numerically verifying the existence of the LM on the microstrip and determining its amplitude.

## II. Background

### A. Leaky Dominant Mode on Microstrip Line

Microstrip line on an isotropic substrate is known to have interesting leakage properties in that the conventional bound dominant mode does not leak at any frequency, while a leaky dominant mode is found to exist at higher frequencies in addition to the BM [16]. The leaky dominant mode has a quasi-TEM current distribution across the strip width that closely resembles that of the BM and, hence, this LM may be excited strongly by a typical feed or discontinuity on the line, when the LM is present and is physical. An example of the behavior of the dominant LM on microstrip is shown in Fig. 3, where the strip width to substrate ratio $w/h$ is unity, and the substrate relative permittivity is $\varepsilon_r = 2.2$. One can see that above a certain frequency, an LM, shown as the solid curve, is present simultaneously with the BM, which appears as the dashed curve. The LM curve begins at a normalized frequency $h/\lambda_0 = 0.091$, while below that frequency, the LM is replaced by a pair of improper real solutions (improper solutions having a real propagation constant), shown in gray, which are nonphysical. The frequency at which the LM solution joins the two improper real solutions is called the "splitting point" [13]. Although leakage first begins at the splitting point (an LM with a complex wavenumber emerges at this frequency), the LM is nonphysical at this point.

Between the splitting point and frequency at which the LM curve and $\mathrm{TM}_0$ surface-wave curve (shown as a dotted curve) cross, i.e., at about $h/\lambda_0 = 0.108$, the LM is slow with respect to the surface wave, rather than fast. In this region, the leaky-wave pole is not captured in a steepest descent analysis of the current excitation from a practical source on the printed-circuit line. This frequency range is, therefore, in the "spectral gap" and the LM in this frequency region is only partly physical. For frequencies greater than that crossing, where the LM is a fast wave with respect to the surface wave, the LM pole is captured and the LM is physical.

### B. Dispersion Curve for the Surface Wave

Surface waves on a dielectric substrate are known to be very dispersive when they are examined over a wide frequency range, but appear to be rather flat with frequency at low frequencies. When a metallic top cover is placed above the substrate, the surface wave becomes a parallel-plate mode, and the biggest change in the dispersion curve occurs at and near zero frequency. When the top cover is absent, the limit at zero frequency for the value of $k_s/k_0$, where $k_s$ is the surface-wave wavenumber and $k_0$ is the free-space wavenumber, is unity. The addition of a top cover causes the surface-wave mode to become a parallel-plate mode, with a wavenumber $k_{pp}$. With a top cover present, the low-frequency limit for $k_{pp}/k_0$ is no longer unity, but becomes some value between unity and $(\varepsilon_r)^{1/2}$, depending on the filling factor of the dielectric layer between the top and bottom plates. If the top cover is placed ***nearer*** to the dielectric layer, the filling factor will increase, and the value of $k_{pp}/k_0$ at zero frequency will ***increase***.

Raising the value of the phase constant for the parallel-plate mode lowers the frequency at which physical leakage can begin since physical leakage occurs when the phase constant of the LM is less than that of the parallel-plate mode. This is demonstrated by the results presented in Section IV. This lowering of the frequency at which physical leakage occurs can result in strong LM excitation as the cover height is reduced, which, in turn, can result in serious spurious transmission effects. This behavior will also be demonstrated clearly in Section IV.

## III. Analysis

### A. Propagation on an Infinite Line

For obtaining the wavenumber behavior of the bound and LMs on a microstrip line, a two-dimensional analysis is sufficient [11], [13], [16]. In this analysis, an infinite line is assumed, with no source. The total surface-current density on the line is represented as

$$J_{sz}(x,z) = T(x)I(z) \tag{1}$$

where the total strip current is

$$I(z) = e^{-jk_z z} \tag{2}$$

and the transverse profile function is taken as

$$T(x) = \frac{1}{\sqrt{\left(\frac{w}{2}\right)^2 - x^2}}. \tag{3}$$

Assuming a perfectly conducting strip, the electric-field integral equation (EFIE) requires zero tangential field on the strip. The EFIE is enforced using Galerkin's method in the spectral domain, yielding a transcendental equation for the unknown wavenumber $k_z = \beta - j\alpha$ of the form

$$\int_{C_x} \tilde{G}_{zz}(k_x, k_z)\tilde{T}^2(k_x)\, dk_x = 0 \tag{4}$$

where $\tilde{G}_{zz}$ is the $zz$ component of the spectral-domain Green's function for the layered parallel-plate structure and $C_x$ is an appropriate path from minus infinity to infinity in the complex $k_x$-plane. A path along the real axis yields the wavenumber for a bound mode, as in a customary spectral-domain analysis. To determine the wavenumber of an LM, one must in addition detour around the pole or poles of the parallel-plate structure [11], [13], [16].

The above procedure has been explained for a single basis function $T(x)$ of longitudinal current for simplicity, although the method is easily generalized to include a transverse current component, and to allow for multiple basis functions across the width of the strip, for both the longitudinal and transverse currents [11]. Results have shown that a single basis function $T(x)$ is accurate for small strip widths, although all results shown later are generated using multiple basis functions for both the longitudinal and transverse current components, in order to have the highest possible accuracy.

### *B. Current Excited by a Delta-Gap Source*

Fig. 2 shows an infinite microstrip line excited by a 1-V delta-gap source on the line. The theory for calculating the current $I(z)$ on the line due to the delta-gap source has been discussed in detail in [18] and [19], thus, only an overview is given here. As in the previous discussion, the calculation procedure will be illustrated for a single basis function $T(x)$ of longitudinal current for simplicity, but in the actual implementation, multiple basis functions of longitudinal and transverse current were actually used.

The current is represented by (1), where the total strip current $I(z)$ may have an arbitrary variation with distance $z$. In the spectral domain, it is possible to solve directly for the Fourier transform of the strip current $\tilde{I}(z)$ by applying a Galerkin testing procedure to the EFIE, which states that

$$\int_{-\infty}^{\infty}\int_{-\infty}^{\infty} G_{zz}(x-x', z-z')J_{sz}(x', z')\, dx'\, dz' = E_z^{\text{gap}}(x, z) \tag{5}$$

where $E_z^{\text{gap}}(x, z)$ is the impressed field of the delta-gap source, chosen to be of the form $T(x)E_z^{\text{gap}}(z)$. Ideally, the function $E_z^{\text{gap}}(z)$ is a delta function, although in numerical implementation, a finite-width pulse function (with width $0.1\lambda_0$) is assumed, to make the Fourier transform converge faster. Omitting further details [18], the Fourier transform of the current is

$$\tilde{I}(k_z) = \frac{2\pi\tilde{E}^{\text{gap}}(k_z)}{\displaystyle\int_{C_x} \tilde{G}_{zz}(k_x, k_z, h)\tilde{T}^2(k_x)\, dk_x}. \tag{6}$$

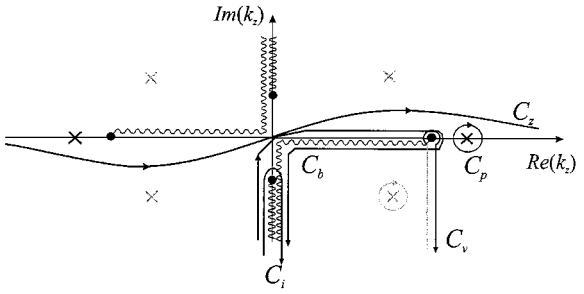


Fig. 4. Paths of integration in the complex $k_z$-plane that are used to calculate the total strip current and its constituent components (see Section III-B) for a covered microstrip line.

The total strip current is then obtained by numerically performing the inverse transform in the $k_z$-plane

$$I(z) = \frac{1}{2\pi}\int_{C_z} \tilde{I}(k_z)e^{-jk_z z}\, dk_z \tag{7}$$

where $C_z$ is a Sommerfeld-type path from minus infinity to infinity that detours around pole and branch-point singularities on the real axis in the $k_z$-plane.

An in-depth discussion of the complex $k_z$-plane for the integration in (7) is given in [12], [18], and [19]. Only the salient features necessary for understanding the results are summarized here. The original path of integration $C_z$ in the $k_z$-plane for (7) is along a Sommerfeld path, as shown in Fig. 4. Branch points in the $k_z$-plane appear at the wavenumbers of the parallel-plate modes. Assuming only one parallel-plate mode (i.e., the $\text{TM}_0$ mode) to be above cutoff, there is only one pair of branch points on the real $k_z$-axis. The branch point are at $k_z = \pm k_{\text{TM}_0}$, where $k_{\text{TM}_0}$ is the wavenumber of the $\text{TM}_0$ mode. An infinite number of branch points appear on the imaginary axes, corresponding to evanescent parallel-plate modes. Poles in the $k_z$-plane correspond to modes of propagation on the microstrip line. Poles corresponding to BMs of propagation occur on the real axis (the $\times$ symbol in Fig. 4). LM poles lie in the complex plane, in the second and fourth quadrants. The LM poles lie on the lower sheet of the $k_{\text{TM}_0}$ branch points, and are shown with gray $\times$ symbols in Fig. 4. (For lossless structures, conjugate poles also lie in the first and third quadrants, corresponding to nonphysical modes that grow with distance along the transmission line. These poles will be ignored.) LM poles in the fourth quadrant that correspond to physical fast waves lie to the left-hand side of the branch point $k_{\text{TM}_0}$, while poles to the right-hand side of the branch point correspond to slow-wave LMs that are in the spectral gap. The further into the spectral-gap (to the right-hand side of the branch point) an LM pole is, the less physical the LM is.

The original path $C_z$ may be deformed into a path that circles the BM on the positive real axis and a path that encircles all of the branch cuts, as shown by the paths $C_p$ and $C_b$ in Fig. 4. The first path yields a residue contribution that defines the launching amplitude of the BM from the delta-gap source. The path $C_b$ defines the CS current on the line, which corresponds physically to a radiation field produced by the source.

The CS current can be further resolved by deforming the path $C_b$ to the set of two vertical paths $C_i$ and $C_v$ shown in Fig. 4. The path $C_v$ is a steepest descent path (SDP) that allows for a convenient asymptotic evaluation of the current on the line as the distance from the source increases [23]. The left-hand side of this

path is on the lower sheet of the $k_{\mathrm{TM}_0}$ branch point, while the right-hand-side part is on the top sheet. The contribution from this path is termed the RW current. It is shown in [23] that this contribution behaves asymptotically as $\exp(-jk_{\mathrm{TM}_0}z)/z^{3/2}$. The path $C_i$ yields a current that is the sum of exponentially decaying waves, corresponding physically to a decaying near-field current produced by the source. This current is usually small enough to be ignored at any practical distance from the source. During the deformation of the path $C_b$, an LM pole will also be captured if it is in the fast-wave (physical region). Fig. 4 shows an LM pole that has been captured, with a corresponding path (in gray) on the lower sheet that encircles the pole. The residue contribution is used to define the launching amplitude of the LM. Hence, the CS current can be written as the sum of any physical LMs and the RW current, along with a rapidly decaying near-field current (which will be neglected in the remaining discussions). The RW current represents that portion of the CS that is not represented by the LM, and corresponds primarily to direct radiation from the source, observed along the strip conductor.

Although the decomposition of the CS current into its constituent parts is not unique, the method described above is simple and direct, and it allows for a convenient asymptotic evaluation of the RW current [23].

If the LM is in the spectral-gap region, the corresponding pole is not captured by the path deformation to the SDP. In accordance with the definition used here for the RW current, the CS current is then simply the RW current. A more sophisticated definition of the RW and LM currents when the LM is in the spectral gap would include a transition function to account for the gradual loss of physical validity of the LM as it enters the spectral-gap region and then approaches the splitting point.

### *C. GPOF Method*

The GPOF method [24] is a convenient tool that aids in quantifying the physical validity of the LM [18], [21]. The current on the line is sampled and then approximated by a sum of exponential functions having different amplitudes and wavenumbers. If the actual current on the line produced by the source has a significant LM component, the LM should appear distinctly in the GPOF results. A good match between the LM wavenumber and amplitude defined by the residue calculation and the GPOF method is an indication that the LM has a high degree of physical validity. Lack of agreement usually indicates little physical validity.

## IV. RESULTS

### *A. Influence of a Top Cover on the Frequency at Which Leakage Begins*

It was mentioned in Section I that the top cover has the effect of lowering the frequency of the onset of leakage, and that this effect is particularly pronounced for microstrip line. These statements are verified by plotting the dispersion curves for various cover heights. Fig. 3 shows the dispersion plot for a cover height of infinity (regular microstrip). Fig. 5 presents dispersion plots for the same low-permittivity substrate ($\varepsilon_r = 2.2$) and strip-width-to-substrate-height ratio ($w/h = 1.0$) for cover heights of $h_c/h$ 2.0, 1.0, and 0.5, showing the changes in the dispersion plots as the top cover is brought successively nearer to the strip.

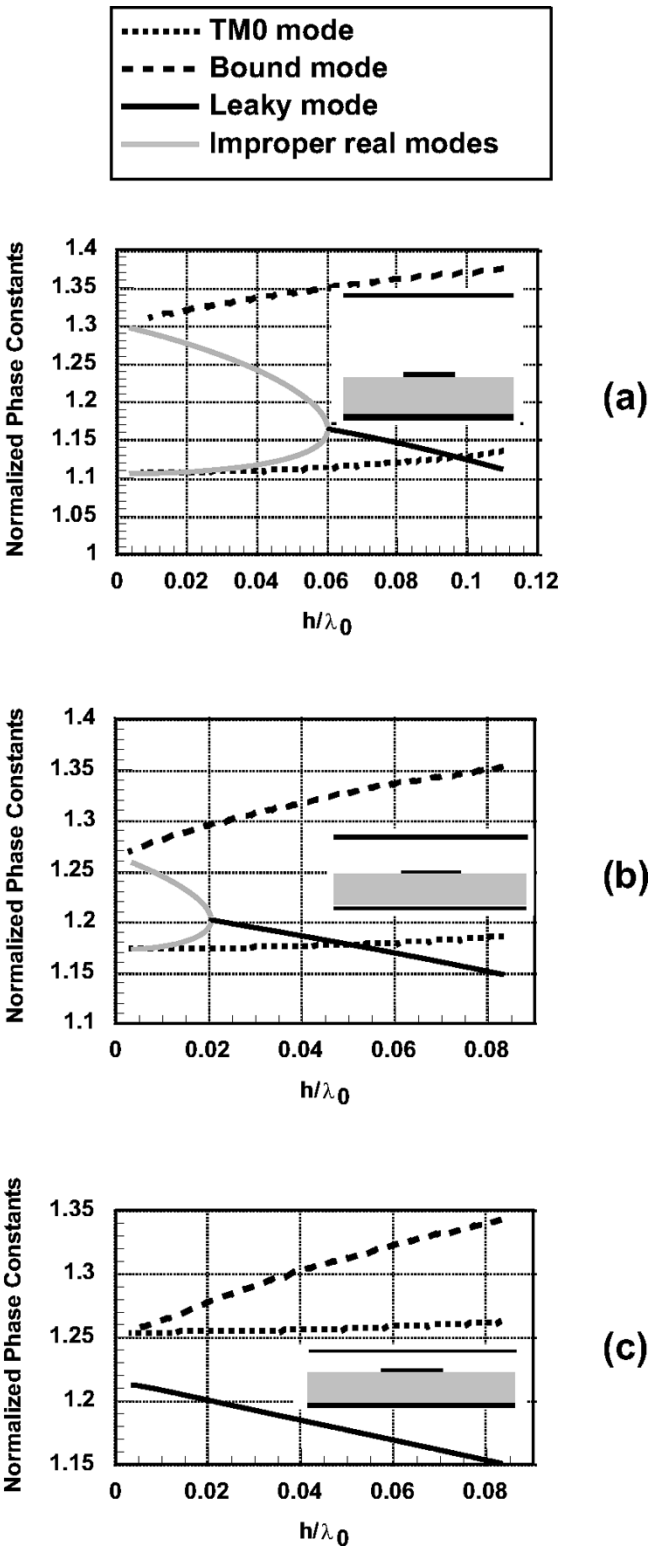


Fig. 5. Dispersion plot for a covered microstrip line showing the normalized phase constant $\beta/k_0$ versus normalized frequency $h/\lambda_0$ for different cover heights. The substrate relative permittivity is $\varepsilon_r = 2.2$ and the strip-width-to-substrate ratio is $w/h = 1.0$. The cover heights are: (a) $h_c/h = 2.0$, (b) $h_c/h = 1.0$, and (c) $h_c/h = 0.5$. We observe that the frequency at the onset of leakage is lowered dramatically as the cover height is reduced.

For the uncovered microstrip, the splitting point (the frequency at which leakage first begins as a nonphysical LM) is at about $h/\lambda_0 = 0.09$, and the frequency at which the LM enters the physical fast-wave region is at about $h/\lambda_0 = 0.11$. Clearly, physical leakage on typical microstrip lines occurs only for high frequencies or thicker substrates. From Fig. 5, we can see that the onset of leakage (the splitting-point frequency) drops dramatically as the top cover gets close to the strip. For a cover height $h_c/h = 1.0$, the frequency at which leakage begins is approximately 0.02. When the cover height is reduced still further to $h_c/h = 0.5$, leakage now occurs at ***all*** frequencies. The case of $h_c/h = 0.5$ may be a bit severe for a practical situation, but it is included to show that it is possible to have leakage at all frequencies due to the influence of a top cover. The results in Fig. 5 clearly demonstrate that, for smaller cover heights, the potential exists for spurious effects such as crosstalk and power loss due to the LM by itself.

Results in the Section IV-B verify the presence of the LM by direct calculation of the strip current, and also show that interference effects (sometimes striking) can arise along the strip due to the simultaneous presence of the BM and LM. For frequencies for which the LM is only partly physical or is not present, the RW can be large enough in some cases to cause significant spurious ripples in the total current along the strip, as is also shown in the Section IV-B.

Fig. 6 shows the same type of results as those in Figs. 3 and 5, for a high-permittivity substrate ($\varepsilon_r = 10.2$). One of the interesting aspects is that the frequency at which leakage begins on the uncovered high-permittivity microstrip [see Fig. 6(a)] is lower than the corresponding frequency for the low-permittivity substrate (Fig. 3), ($h/\lambda_0 = 0.056$ in Fig. 6(a) versus $h/\lambda_0 = 0.090$ in Fig. 3). As the cover height is lowered, the frequency at which leakage begins is also lowered, as for the low-permittivity case. However, the effect of the cover on lowering the leakage frequency is more dramatic for the low-permittivity case. In the high-permittivity case, the splitting point is lowered to $h/\lambda_0 = 0.013$ when the cover height is been brought very close to the substrate at $h_c/h = 0.5$ [see Fig. 6(c)]. The same cover height lowered the leakage frequency in the low-permittivity case sufficiently that leakage occurs at all frequencies [see Fig. 5(c)]. Hence, leakage effects due to a top cover are expected to be more pronounced for low-permittivity substrates. Results shown in Section IV-B for the strip current will confirm this.

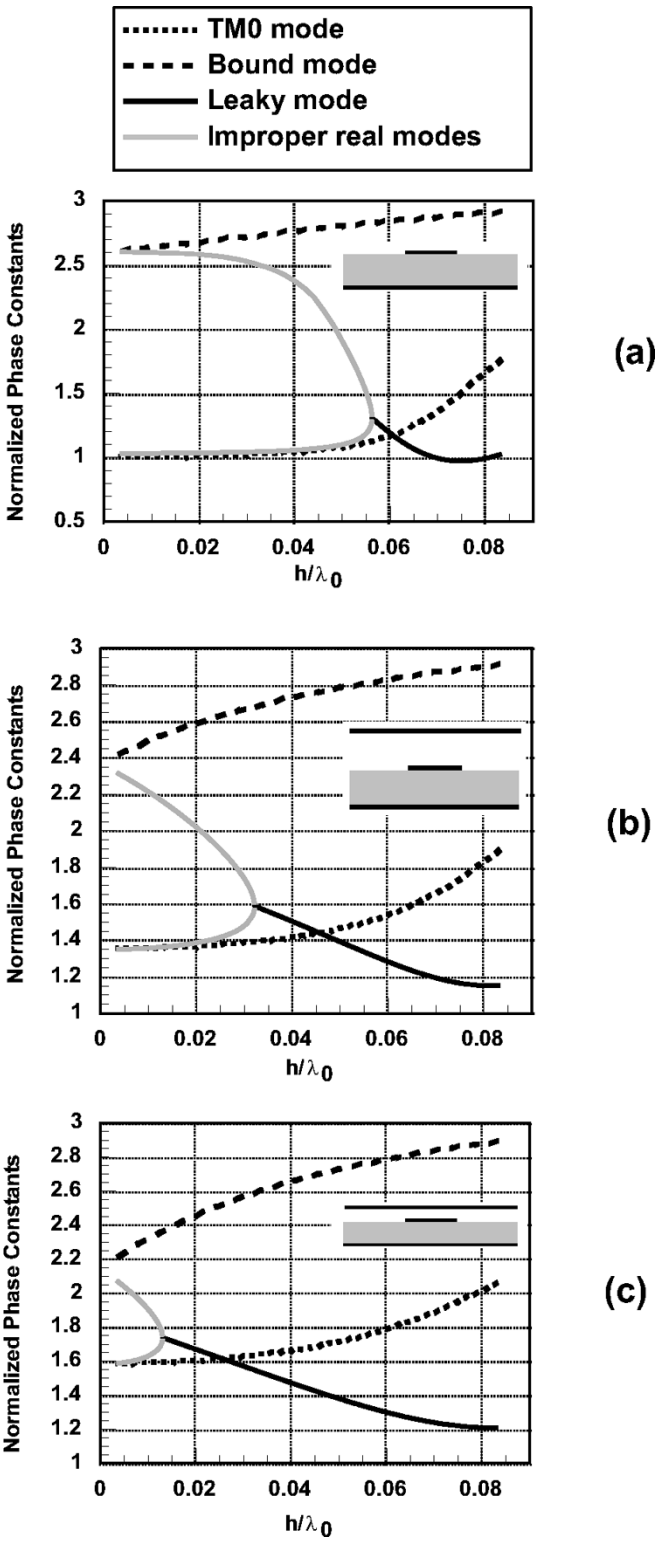


Fig. 6. Same type of dispersion plot as in Figs. 3 and 5, but for a higher permittivity substrate having a relative permittivity of $\varepsilon_r = 10.2$. The dispersion plots show the normalized phase constant $\beta/k_0$ versus normalized frequency $h/\lambda_0$ for different cover heights, with $w/h = 1.0$. The cover heights are: (a) $h_c/h = \infty$, (b) $h_c/h = 1.0$, (c) $h_c/h = 0.5$. The effect of the top cover on lowering the leakage frequency is seen to be less strong when the values of substrate permittivity are high.

### *B. Strip Current from a Source Excitation*

The total current on the line due to the 1-V delta-gap source (Fig. 2) has been calculated by using the method described in Section III, and the total current has been separated into the BM and CS components. Plots showing the various currents versus distance from the source are quite helpful in assessing the degree of spurious transmission effects due to the CS, and in showing the role (or lack thereof) of the LM in determining the CS.

Fig. 7 shows a plot of the current for the low-permittivity case of Fig. 3 for several different cover heights and normalized frequencies. In Fig. 7(a), results are first shown for uncovered microstrip (cover height of infinity) at a moderate frequency of $h/\lambda_0 = 0.04$. At this frequency, we may note from Fig. 3 that there is no LM, thus, the CS consists only of the RW. From Fig. 7(a), we see that the CS current is very small, and that the total strip current is essentially the same as that of only the BM.

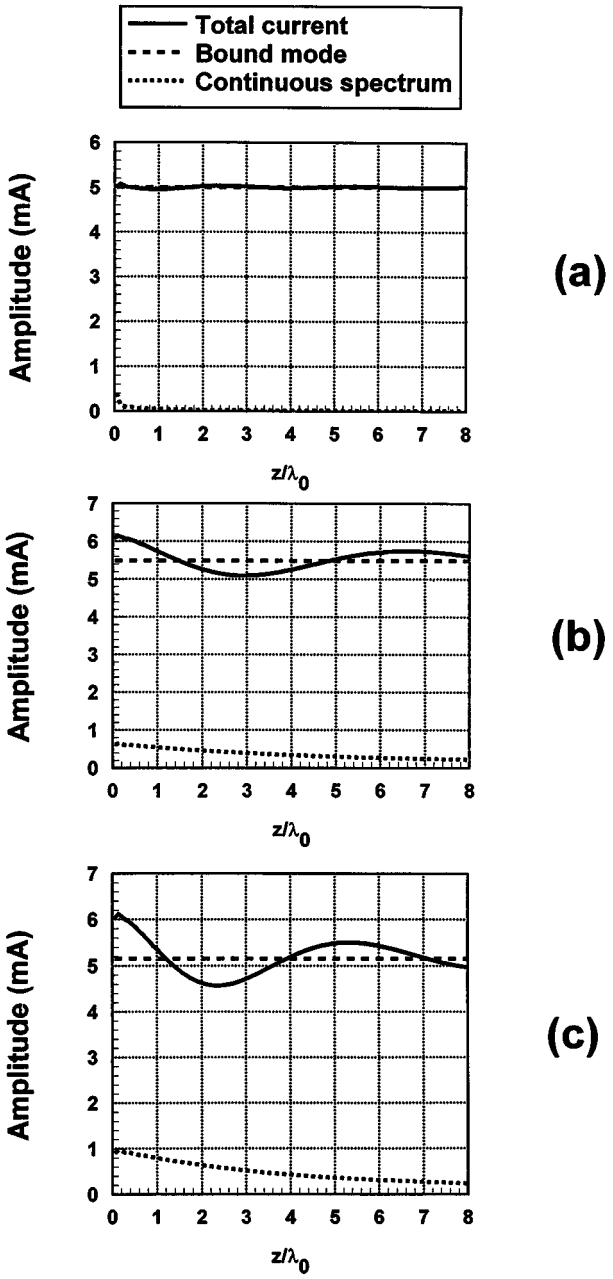


Fig. 7. Plots of the total current, BM current, and CS current on a microstrip line versus normalized distance from the delta-gap voltage source, for different cover heights $h_c/h$ and different normalized frequencies $h/\lambda_0$. For all cases, $\varepsilon_r = 2.2$ and $w/h = 1.0$. The other parameters are: (a) $h/\lambda_0 = 0.04$ and $h_c/h = \infty$, (b) $h/\lambda_0 = 0.02$ and $h_c/h = 1.0$, (c) $h/\lambda_0 = 0.04$ and $h_c/h = 1.0$. For cases (a) and (b), there is no LM present, whereas for case (c), the LM is only partly physical because it is within the spectral gap. These curves show that the level of spurious interference effects increases with increasing frequency and with decreasing cover height.

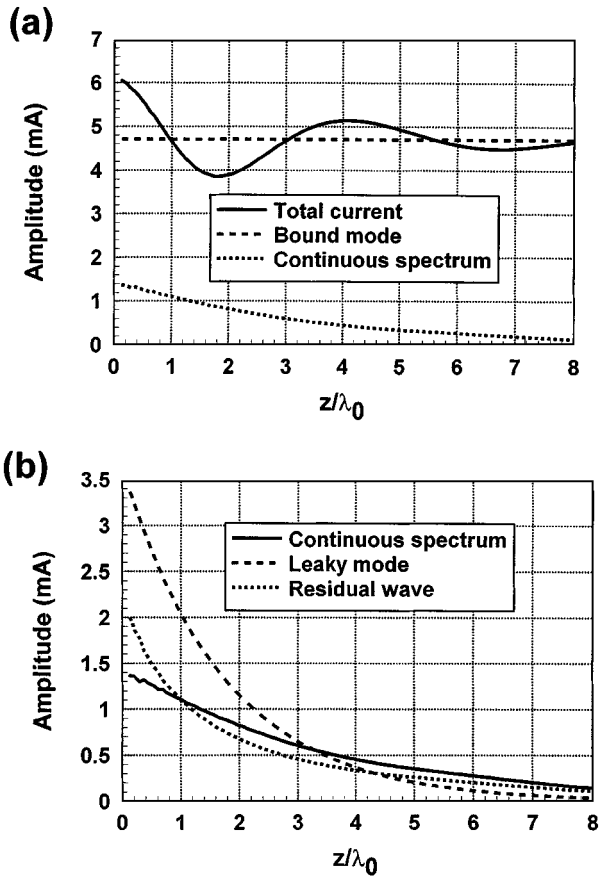


Fig. 8. (a) Same type of plot as in Fig. 7(b) and (c), for the same covered microstrip structure, except that the normalized frequency has been increased to $h/\lambda_0 = 0.08$. (b) The CS current is shown along with its constituent parts: the LM current and the RW current. At this higher frequency, the LM is fully physical.

The RW is, therefore, very small. At this moderate frequency, the CS is small enough that no serious spurious effects are observed.

Fig. 7(b) and (c) shows plots of the current for the same low-permittivity case as in Fig. 7(a), but for a moderate cover height of $h_c/h = 1.0$. In Fig. 7(b), the normalized frequency is $h/\lambda_0 = 0.02$ [half of the value used in part Fig. 7(a)], while in Fig. 7(c), the normalized frequency is $h/\lambda_0 = 0.04$ [the same as that used in Fig. 7(a)]. In Fig. 7(b), the leakage first begins [at the splitting point in Fig. 5(b)] as a nonphysical LM. In Fig. 7(c), the LM is only partly physical because it is in the spectral-gap region. In each, the total current is shown along with its constitutive parts: the BM and CS currents.

The results in Fig. 7(b) and (c) show that the amplitude of the BM remains fairly constant with frequency (which is expected since the characteristic impedance of the BM changes gradually with frequency and the voltage at the source remains constant) and that the CS current increases monotonically in amplitude as the frequency increases. The total current clearly shows an oscillation effect due to inference between the BM and CS currents. The level of this oscillation increases with frequency along with the CS current. Clearly, spurious transmission effects due to the CS current can occur with a moderate cover height at moderate frequencies. However, the CS current is often not dominated by the LM. This is evident from Fig. 7(b) and (c), where the LM is either not present at all [see Fig. 7(b)] or is in the spectral gap where it is only partly physical [see Fig. 7(c)], but we see that oscillations of the total current along the line are clearly present.

Fig. 8 shows plots of the current for the same structure as in Fig. 7(b) and (c), where the normalized frequency has been increased to $h/\lambda_0 = 0.08$. For this frequency, the LM is well within the physical region [see Fig. 5(b)]. At this higher frequency, the amplitude of the CS current and, hence, the level

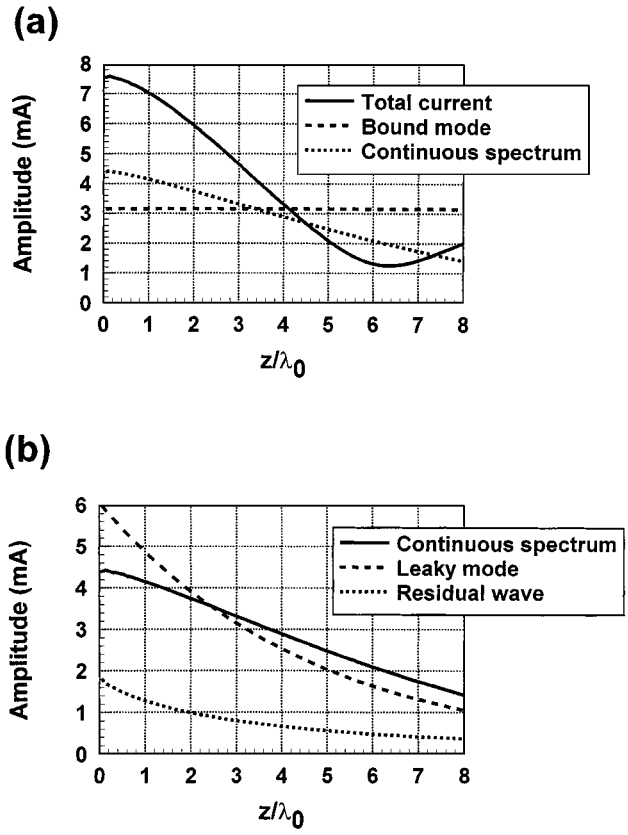


Fig. 9. (a) Plot of the total current, BM current, and CS current on a covered microstrip line versus distance from the delta-gap voltage source, for $\varepsilon_r = 2.2$, $w/h = 1.0$, and a cover height of $h_c/h = 0.5$. The normalized frequency is $h/\lambda_0 = 0.02$. (b) The CS current is shown along with its constituent parts: the LM current and the RW current. The LM now dominates the CS, and the interference effect is very strong.

TABLE I
NORMALIZED WAVENUMBER VALUES ($k_z/k_0$) FOR THE BM AND LM, AND THE AMPLITUDES OF THE BOUND AND LEAKY MODES, RESPECTIVELY, FOR THE CASE SHOWN IN FIG. 9. $\varepsilon_r = 2.2$, $w/h = 1.0$, AND $h_c/h = 0.5$ AT A NORMALIZED FREQUENCY OF $h/\lambda_0 = 0.02$. THE WAVENUMBER AND AMPLITUDE VALUES ARE CALCULATED IN TWO WAYS: 1) FROM THE LEAKY-MODE POLES IN THE COMPLEX PLANE (THEORY) AND 2) A NUMERICAL GPOF PROCEDURE. THE WAVENUMBER OF THE $\mathrm{TM}_0$ PARALLEL-PLATE MODE IS ALSO SHOWN FOR CONVENIENCE

| Mode | Normalized propagation constants | | | | Amplitude [mA] | |
|---|---|---|---|---|---|---|
| | Theory | | GPOF | | Theory | GPOF |
| | $\beta/k_0$ | $\alpha/k_0$ | $\beta/k_0$ | $\alpha/k_0$ | | |
| Bound Mode | 1.277 | 0 | 1.283 | 0.003 | (-3.15, 0) | (-2.78, -0.99) |
| Leaky Mode | 1.201 | 0.035 | 1.195 | 0.032 | (-5.48, 0.95) | (-4.94, 0.94) |
| $TM_0$ | 1.254 | 0 | - | - | - | - |

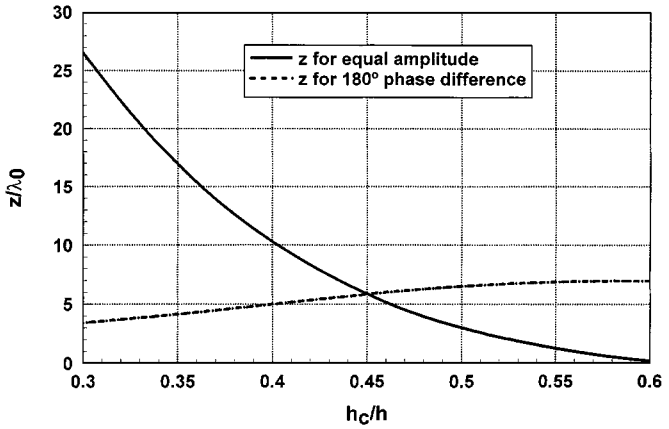


Fig. 10. One curve shows the normalized distance $z/\lambda_0$ from the delta-gap source at which the BM and CS currents are equal in magnitude versus the normalized cover height. The other curve shows the normalized distance for which there is a 180° phase difference between the BM and CS currents. The results are for the case $\varepsilon_r = 2.2$ and $h/\lambda_0 = 0.02$.

of the spurious oscillations, have increased from what was observed in Fig. 7. Although the LM is now physical at this higher frequency, Fig. 8 shows that the amplitudes of the LM and RW currents are roughly the same order of magnitude. Hence, even though spurious transmission effects continue to increase with frequency, and become even stronger in the region where a physical LM is present, the spurious effects are not exclusively an LM effect, but are still caused to a large extent by the RW current.

Fig. 9 shows the currents for the case of a smaller cover height, $h_c/h = 0.5$, at the frequency $h/\lambda_0 = 0.02$ (see Fig. 5(c) for the wavenumber plot). All other parameters remain the same as those in Figs. 7 and 8. Fig. 9 reveals two important aspects about the effects of reducing the cover height. First, the level of oscillation in the total current has increased significantly, compared to that in Fig. 7(b), which corresponds to the same frequency. This is because lowering the cover height has decreased the amplitude of the BM and, more importantly, it has dramatically increased the amplitude of the CS current. Second, Fig. 9(b) shows that the LM is now the main component of the CS current. Comparing Figs. 7(b) and 9, it is also seen that the RW current is somewhat stronger for the lower cover height. (Note that, in Fig. 7(b), there is no physical LM present, so that the RW current is the same as the CS current.) However, the main reason the CS current is significantly larger in Fig. 9 is the presence of the very strong LM. Hence, when the cover is brought near to the substrate, a very strong physical LM is excited, which dominates the CS current and produces very significant oscillations in the total current. It should also be noted that these effects are occurring at a rather low frequency.

Table I compares the values of wavenumber and amplitude for the BM and LM (with the wavenumber of the $\mathrm{TM}_0$ parallel-plate mode also shown for convenience) for the case shown in Fig. 9. The "Theory" values come from the BM and LM poles in the $k_z$-plane. In particular, the wavenumbers are determined directly by the location of the poles, while the amplitudes of the modes are determined from (7) by the residues at the poles. The "GPOF" values represent the wavenumbers and amplitudes of the exponential current waves that the GPOF method yields from the numerical fit to the sampled current on the line. The table shows reasonable agreement for both the wavenumber and amplitude between the residue results and GPOF results. The good agreement for the BM is expected since the BM is a discrete proper modal solution that is present on the line. The good agreement for the LM is evidence that the LM is a significant part of the CS current, which confirms the result in Fig. 9.

For a particular cover height, a perfect destructive interference between the BM and CS currents can be observed. Such drastic cancellation effects can be obtained only if the amplitude

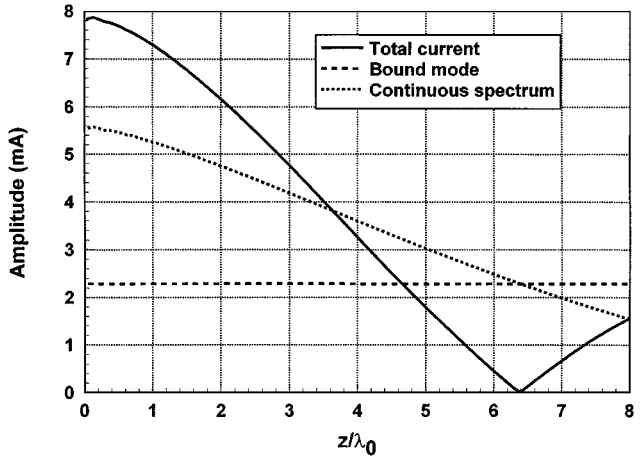


Fig. 11. Plot of the total current, BM current, and CS current versus normalized distance for a covered microstrip case having $\varepsilon_r = 2.2$, $w/h = 1.0$, $h_c/h = 0.455$, and $h/\lambda_0 = 0.02$. For this critical cover height, there is a perfect destructive interference between the BM and CS currents that occurs at approximately $z/\lambda_0 = 6.4$.

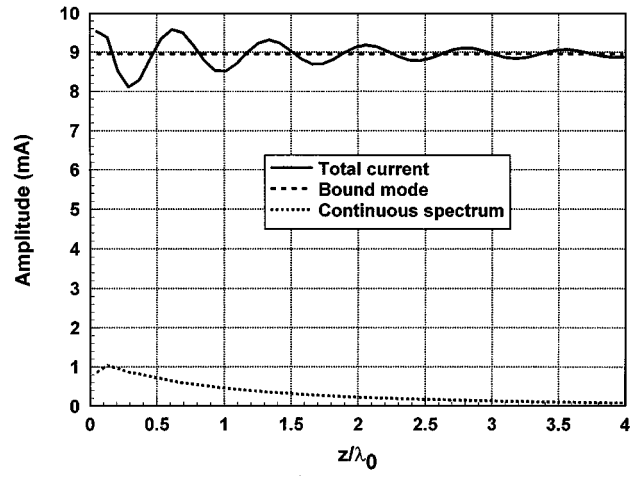


Fig. 12. Plot of the total current, BM current, and CS current versus normalized distance for a high-permittivity covered microstrip case having $\varepsilon_r = 10.2$ with $w/h = 1.0$, $h_c/h = 1.0$, and $h/\lambda_0 = 0.04$. The interference effects are less strong when the substrate permittivity is higher.

of the CS current excited at the source is greater than that of the BM current, because the BM current amplitude remains constant with $z$, while the CS current decreases with $z$. To see how such an effect can be realized, Fig. 10 shows a plot of the normalized distance from the source, versus the normalized cover height, at which the BM and CS currents are equal in magnitude. Another plot on the same figure shows the normalized distance at which the phase difference between the BM and CS currents is 180°. The cover height corresponding to the crossing of the two plots determines a critical cover height $h_c/h = 0.455$ for which perfect destructive interference between the BM and CS currents occurs (at a distance $z/\lambda_0 = 6.4$ given by the vertical axis coordinate of the intersection point). Fig. 11 shows a plot of the current versus distance for this critical cover height, verifying that a perfect null in the total current is obtained. Since the LM current dominates the CS current (similar to the case of Fig. 9), the null is mainly due to an interference between the BM and LM currents. Obviously, this type of interference would be disastrous for circuit performance.

Fig. 12 shows plots of current versus distance for the high-permittivity case of Fig. 6(b) ($\varepsilon_r = 10.2, h_c/h = 1.0$), at $h/\lambda_0 = 0.04$. Comparing with Fig. 7(c), it is concluded that the level of oscillations in the total current at a given frequency is less for a high-permittivity substrate. This is because the BM current is larger for the high-permittivity case (due to the lower characteristic impedance of the line), while the CS current is smaller (at least for moderate distance from the source). Hence, less serious spurious effects will generally occur when using higher permittivity substrates.

## V. Conclusions

A leaky dominant mode can exist on microstrip line without a top cover, but only for relatively high frequencies (or thick substrates). However, when a top cover is introduced over the substrate, the frequency at which leakage begins is dramatically ***lowered***. In fact, when the top cover is brought sufficiently near to the strip, the microstrip line becomes leaky at all frequencies. This leakage can produce crosstalk between constituent parts of an integrated circuit, and power loss along the line. Since the conventional BM is always present at the same time, interference effects can also arise in the total current along the line. Curves have been presented in Section IV for several values of cover height over a wide range of frequencies, and these major points were illustrated there.

The amplitude of the LM that is excited by a delta-gap source on the line was examined in order to assess the level of spurious (interference) transmission effects on a practical microstrip line that could be caused by the LM. Various examples of spurious transmission effects have been presented in a series of curves (in the form of strip current versus distance along the strip) for different cover heights, permittivity values, and frequencies. A numerical method called the GPOF method was used to further characterize the physical behavior of the LM that is excited on the line by the source.

In addition to the BM and LM currents, the total current on the line produced by the source includes an RW current, which may be interpreted physically as the direct radiation from the source observed along the strip. The LM and RW currents together make up the CS current produced by the source. The RW current is important because it can also be responsible for spurious effects, especially in those cases when there is no physical LM.

A specific summary of the new features that have been discovered as a result of this study, and verified with numerical results, are as follows.

1) A top cover placed above a circuit utilizing microstrip line significantly lowers the frequency at which leakage begins. When the top cover is very near to the strip, this reduction in frequency can be so dramatic that the leakage will occur at all frequencies.
2) Corresponding behavior involving CPW was reported recently [22], but the lowering of the frequency for leakage is much more pronounced for microstrip line.

3) The effect of the top cover on lowering the leakage frequency is less strong when the values of substrate permittivity are high.
4) Another important difference between the CPW and microstrip cases is that, for CPW, the dominant (bound) mode changes into an LM above some critical frequency, whereas for microstrip line, the LM is present in addition to the conventional BM. Both lines will suffer from crosstalk and power-loss problems when leakage occurs, but, because the leaky and BMs are present simultaneously for microstrip line, it will encounter an additional important effect. These two modes launched by the source will interfere with each other and produce spurious variations in the amplitude of the total current along the line.
5) The amplitude of the LM excited by the source increases as the top cover is placed nearer to the strip. For cover heights equal to or less than the substrate thickness, the amplitude of the LM may be comparable to that of the BM. In this latter situation, the interference effects can become very pronounced and, for a particular cover height, complete cancellation occurs and a null in the current is obtained at a certain distance from the source. This occurs when the cover height is roughly half of the substrate thickness. This cancellation effect would be disastrous for circuit performance.
6) The total current excited by the source includes the effects of direct radiation from the source (i.e., RW), as well as LM excitation. This direct source radiation can significantly affect the behavior of the total current, causing interference effects similar to that produced by the LM. The direct source radiation was found to be very small when there is no top cover, but to increase strongly as the cover height is reduced, producing significant interference oscillations in the total current along the line. This effect may occur even for frequencies for which the LM does not exist, and is something new to watch out for when a top cover is introduced.

## REFERENCES


[1] A. Oliner and K. S. Lee, "The nature of leakage from higher-order modes on microstrip lines," in *IEEE MTT-S Int. Microwave Symp. Dig.*, Baltimore, MD, June 1986, pp. 57–60.

[2] H. Shigesawa, M. Tsuji, and A. A. Oliner, "Conductor-backed slotline and coplanar waveguide: Dangers and full-wave analysis," in *IEEE MTT-S Int. Microwave Symp. Dig.*, New York, NY, May 1988, pp. 199–202.

[3] M. Tsuji, H. Shigesawa, and A. A. Oliner, "Printed circuit waveguides with anisotropic substrates: A new leakage effect," in *IEEE Int. Microwave Symp. Dig.*, Long Beach, CA, June 1989, pp. 783–786.

[4] A. A. Michalski and D. Zheng, "Rigorous analysis of open microstrip lines of arbitrary cross section in bound and leaky regions," *IEEE Trans. Microwave Theory Tech.*, vol. 37, pp. 2005–2010, Dec. 1989.

[5] N. K. Das and D. M. Pozar, "Full-wave spectral-domain computation of material, radiation, and guided wave losses in infinite multilayered printed transmission lines," *IEEE Trans. Microwave Theory Tech.*, vol. 39, pp. 54–63, Jan. 1991.

[6] H. Shigesawa, M. Tsuji, and A. A. Oliner, "Dominant mode power leakage from printed-circuit waveguides," *Radio Sci.*, vol. 26, no. 1, pp. 559–564, Mar.–Apr. 1991.

[7] M. Tsuji, H. Shigesawa, and A. A. Oliner, "Simultaneous propagation of bound and leaky dominant modes on printed-circuit lines," *IEEE Trans. Microwave Theory Tech.*, vol. 43, pp. 3007–3019, Dec. 1995.

[8] D. P. Nyquist, J. S. Bagby, C. H. Lee, and Y. Yuan, "Identification of propagation regimes on integrated microstrip transmission lines," *IEEE Trans. Microwave Theory Tech.*, vol. 41, pp. 1887–1893, Nov. 1993.

[9] D. Nghiem, J. T. Williams, D. R. Jackson, and A. A. Oliner, "Proper and improper dominant mode solutions for stripline with an air gap," *Radio Sci.*, vol. 28, no. 6, pp. 1163–1180, Nov.–Dec. 1993.

[10] H. Shigesawa, M. Tsuji, and A. A. Oliner, "The nature of the spectral gap between bound and leaky solutions when dielectric loss is present in printed-circuit lines," *Radio Sci.*, vol. 28, no. 6, pp. 1235–1343, Nov.–Dec. 1993.

[11] F. Mesa and R. Marqués, "Integral representation of spatial Green's function and spectral domain analysis of leaky covered strip-like lines," *IEEE Trans. Microwave Theory Tech.*, vol. 43, pp. 828–837, Apr. 1995.

[12] D. P. Nyquist and D. J. Infante, "Discrete higher-order leaky-wave modes and the continuous spectrum of stripline," *Trans. IEICE*, vol. E78-C, no. 10, pp. 1331–1338, Oct. 1995.

[13] D. Nghiem, J. T. Williams, D. R. Jackson, and A. A. Oliner, "Leakage of the dominant mode on stripline with a small air gap," *IEEE Trans. Microwave Theory Tech.*, vol. 43, pp. 2549–2556, Nov. 1995.

[14] ——, "The effect of substrate anisotropy on the dominant-mode leakage from stripline with an air gap," *IEEE Trans. Microwave Theory Tech.*, vol. 43, pp. 2831–3828, Dec. 1995.

[15] F. Mesa and R. Marqués, "Low-frequency leaky regime in covered multilayered striplines," *IEEE Trans. Microwave Theory Tech.*, vol. 44, pp. 1521–1525, Sept. 1996.

[16] D. Nghiem, J. T. Williams, D. R. Jackson, and A. A. Oliner, "Leakage of the dominant mode on microstrip with an isotropic substrate: Theory and measurements," *IEEE Trans. Microwave Theory Tech.*, vol. 44, pp. 1710–1715, Oct. 1996.

[17] ——, "Existence of a leaky dominant mode on microstrip line with an isotropic substrate: Theory and measurement," *IEEE Trans. Microwave Theory Tech.*, vol. 34, pp. 1710–1715, Dec. 1996.

[18] C. Di Nallo, F. Mesa, and D. R. Jackson, "Excitation of leaky modes on multilayer stripline structures," *IEEE Trans. Microwave Theory Tech.*, vol. 46, pp. 1062–1071, Aug. 1998.

[19] F. Mesa, C. Di Nallo, and D. R. Jackson, "The theory of surface-wave and space-wave leaky mode excitation on microstrip lines," *IEEE Trans Microwave Theory Tech.*, vol. 47, pp. 207–215, Feb. 1999.

[20] F. J. Villegas, D. R. Jackson, J. T. Williams, and A. A. Oliner, "Leakage fields from planar semi-infinite transmission lines," *IEEE Trans. Microwave Theory Tech.*, vol. 47, pp. 443–454, Apr. 1999.

[21] M. Freire, F. Mesa, C. Di Nallo, D. R. Jackson, and A. A. Oliner, "Spurious transmission effects due to the excitation of the bound mode and the continuous spectrum on stripline with an air gap," *IEEE Trans. Microwave Theory Tech.*, vol. 47, pp. 2493–2502, Dec. 1999.

[22] A. A. Oliner, "Package effects caused by leaky modes at higher frequencies in microwave integrated circuits," in *Proc. 29th European Microwave Conf.*, Munich, Germany, Oct. 4–8, 1999.

[23] D. R. Jackson, F. Mesa, M. Freire, D. P. Nyquist, and C. Di Nallo, "An excitation theory for bound modes, leaky modes, and residual-wave current on stripline structures," *Radio Sci.*, vol. ??, pp. 495–510, Mar.–Apr. 2000.

[24] T. P. Sarkar and O. Pereira, "Using the matrix pencil method to estimate the parameters of a sum of complex exponents," *IEEE Antennas Propagat. Mag.*, vol. 37, pp. 48–55, Feb. 1995.



**F. Mesa**, photograph and biography not available at time of publication.

**A. A. Oliner** (M'47–SM'52–F'61–LF'87), photograph and biography not available at time of publication.

**D. R. Jackson** (S'83–M'84–SM'95–F'99), photograph and biography not available at time of publication.

**Manuel J. Freire**, photograph and biography not available at time of publication.